# PROGRESS WITH MULTI-CELL Nb$_3$Sn CAVITY DEVELOPMENT LINKED WITH SAMPLE MATERIALS CHARACTERIZATION[*]

G. Eremeev[1†], C. E. Reece[1], M. J. Kelley[1,2,3], U. Pudasaini[2], J. R. Tuggle[3]

[1]Thomas Jefferson National Accelerator Facility, Newport News, VA 23606, U.S.A.

[2]Applied Science Department, College of William and Mary, Williamsburg, VA 23185, U.S.A.

[3]Materials Science and Engineering Department, Virginia Tech, Blacksburg, VA 24061, U.S.A.

## Abstract

Exploiting both the new Nb$_3$Sn coating system at the Lab and the materials characterization tools nearby, we report our progress in low-loss Nb$_3$Sn films development. Nb$_3$Sn films a few micrometers thick were grown on Nb coupons as well as single- and multi-cell cavities by the Sn-diffusion technique. Films structure and composition were investigated on coated samples and cavity cutouts with characterization tools including SEM/EDS/EBSD, AFM, XPS, SIMS towards correlating film growth and RF loss to material properties and deposition parameters. Cavity coating efforts focused on establishing techniques for coating progressively more complicated RF structures, and understanding limiting mechanisms in coated cavities. Nb$_3$Sn coated 1.5 GHz 1-cell and 1.3 GHz 2-cell cavities have shown quality factors of $10^{10}$ at 4.3 K, with several cavities reaching above E$_{acc}$ = 10 MV/m. The dominant limiting mechanisms were low field quenches and quality factor degradation above 8 MV/m. The surface data indicates a near-stoichiometric Nb$_3$Sn consistent with the transition temperature and gap measurements. The Nb$_3$Sn layer is covered with Nb$_2$O$_5$ and SnO$_2$ native oxides and has little memory of the pre-coating surface.

## INTRODUCTION

Nb$_3$Sn is one of the Nb-Sn compounds that forms when niobium is annealed in the presence of Sn. This phase occurs for Sn concentrations between 18 and 25 % and annealing temperatures between 930 °C and 2130 °C [1]. The phase is superconducting, but the superconducting transition temperature varies from 6 K for the low Sn content to about 18 K for 25 % of Sn [2]. The transition temperature of 18 K for Nb$_3$Sn is almost twice higher than that of niobium, which implies larger energy gap and, hence, lower dissipation in RF fields that of niobium surfaces. As the consequence of larger energy gap, Nb$_3$Sn also has a higher thermodynamic critical field, which leads to a higher superheating field. The lower RF dissipation and higher critical field are the advantages that can be exploited in accelerating structures, which benefit from low dissipation at high fields.

These benefits to SRF cavities were recognized early and already in early 70's several labs pursued Nb$_3$Sn coating for superconducting accelerator cavity applications [3, 4, 5, 6, 7, 8]. The most sustained effort spanned over a decade at Wuppertal University, where several coating chambers were built and coatings under different conditions were explored. These efforts resulted in quality factors above $10^{11}$ and accelerating gradients above 15 MV/m, limited by a strong Q-slope [9]. The cause of the Q-slope was not completely understood, but subsequent investigation showed that the effect is not local and hence could be a fundamental property of Nb$_3$Sn [10].

More recently, Cornell University pursed Nb$_3$Sn coating on Nb cavities in an attempt to replicate and explain Wuppertal results. While the first coated cavity had a high residual resistance, the coating on the second cavity resulted in a high quality factor without significant degradation up to a quench field of E$_{acc}$ = 17 MV/m! [11] This result demonstrates the potential for high fields in Nb$_3$Sn cavities without Q$_0$ degradation.

In 2012 Jefferson Lab was funded to pursue R&D of SRF technologies for high-efficiency 4 K compact accelerating modules. Quality factors of $10^{10}$ at 4 K in 1.5 GHz accelerating cavities shown at Wuppertal suggested potential for high-efficiency 4 K compact accelerating modules. While originally we planned a two heater system exploited by Wuppertal [9] along with a vapor guide [8], we established a coating procedure following the approach explored at Siemens, where researchers coated superconducting structures using Nb cavities as the coating chamber, and Sn and SnCl$_2$ were placed inside the cavity and exposed to the same temperature during coating as the cavity [3]. It is worth noting that some of the 9.5 GHz cavities coated at Siemens had quality factors of 2.3·$10^9$ at B$_{peak}$ = 101 mT at 1.5 K [3]. Assuming quadratic frequency dependence of the surface resistance, one could speculate that there is potential for quality factors of above $10^{11}$ at E$_{acc}$ = 25 MV/m in 1.3 GHz accelerating structures for such a coating configuration.

The paper is organized as the following : the next section describes the coating setup. The RF results section presents test results from the coated cavities. Then, the material studies section shows the surface properties gleaned from the coated surface with analytical instruments.

## COATING DETAILS

The coating system comprises a niobium vacuum coating chamber inside of which the cavities and samples to be coated are placed and the vacuum furnace that brings the coating chamber to the desired temperature. In Fig. 1, the CAD drawing of the coating chamber with a 5-cell 1.5 GHz cavity as a reference is shown on the left. To avoid cross contamination, the coating chamber has its own pumping system, which is independent of the furnace vacuum. In the center and the right pictures in Fig. 1, a 1-cell 1.5 GHz cavity and a 2-cell 1.3 GHz cavities are shown correspondingly after they were coated and removed from the chamber. On the top of the cavities a 11" Nb support plate can be seen. Sn and $SnCl_2$ are placed on the Nb foil that covers the bottom beam tube. Additional details of the coating system were presented elsewhere [12]. The standard temperature
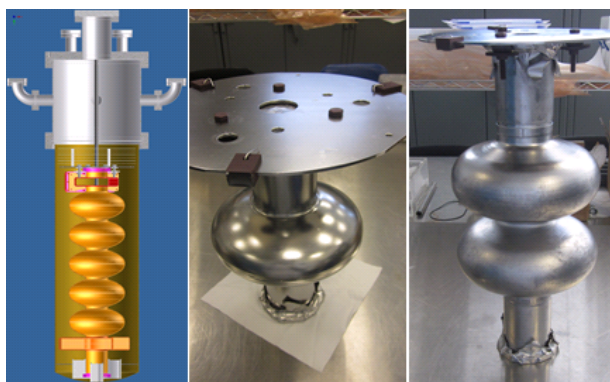


Figure 1: The coating chamber used for coating Nb cavities and coupons [left], coated ALD3 cavity [center], and coated BL1 cavity [right] are shown. The chamber consists of niobium retort with a brazed 14" SS conflat, electropolished SS multiport spool piece, and electropolished SS multiport blank. Inside the chamber a 1.5 GHz 5-cell cavities is shown, with niobium support plate, niobium heat shield, and ceramic hardware. The Nb support plate and niobium foils covering beam tubes can be seen on the cavities in the center and right pictures.

profile, which has been used for all our coatings so far, is shown in Fig. 2. The temperature profile has two plateau regions, at 500 °C for 1 hour and 1200 °C for 3 hours. During the first plateau at 500 °C, which is lower that the melting point of Sn(505 °C) or boiling point of $SnCl_2$(623 °C), but is above the melting point of $SnCl_2$(247 °C), $SnCl_2$ reacts with the niobium surface, and Sn nucleation sites are formed on the surface. The nucleation produces Sn droplets on the surface from few tens of nanometer up to about half a micron size on the surface, Fig. 3 [top left]. By the time the second plateau is reached at 1200 °C Sn vapor deposits on the surface around the nucleation sites and $Nb_3Sn$ grains begin to crystallize on the surface, Fig. 3 [top right]. On the second plateau at 1200 °C, Fig. 2, $Nb_3Sn$ grains continue to grow on the surface in the presence of Sn vapor. One hour at 1200 °C results in the $Nb_3Sn$ grains on the order

of a few hundred nanometers, Fig. 3 [bottom left]. Finally, after 3 hours grains grow to 1-2 $\mu$m in size, Fig. 3 [bottom right]. The resulting surface is usually matte gray in color,
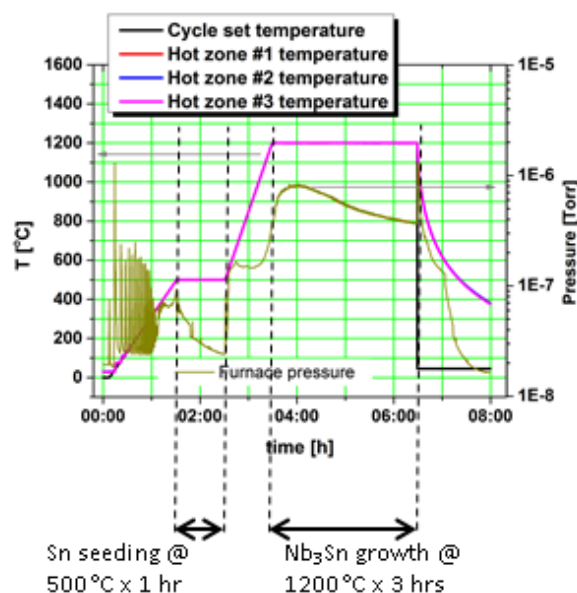


Figure 2: The temperature profile used for coating Nb cavities and Nb coupons. The temperature profile demonstrates the temperature from the three thermocouple located inside the furnace, but outside the coating chamber. The thermocouples are separated vertically by 10", and typically are with ± 1C° during soaks. The vacuum curve shows the vacuum in the furnace, again outside the coating chamber. The vacuum inside the coating chamber is typically about $10^{-5}$ Torr, and increases during the coating run up to about 10 mTorr.

unlike niobium, which is shiny in appearance, Fig. 4. Except for a couple of cases, the coatings resulted in a visually smooth, homogeneous surfaces. The cases, where the coating were not uniform, were reported earlier [13] and are a subject of further research. In this contribution we focused on the coatings that were uniform and were measured with RF techniques and analytic tools.

Besides cavity coatings, several batches of samples were coated in a chamber built for small sample coatings under the same temperature profile. Again, the process resulted in uniformly coated surfaces. The transition temperature of one of the coated samples was found to be 18 K, consistent with cavity measurements.

## RF RESULTS

All cavities for these studies have been previously used in other SRF studies. The single cell cavities were 1.5 GHz CEBAF-shape cavities, which were built with the standard stamp-and-weld technique. We also had four 2-cell seamless cavities made by hydroforming from seamless tubes [14]. The measurement of the transition temperature and the surface resistance as a function of temperature

Fundamentals SRF R&D - Other Materials

D02-Non-niobium films
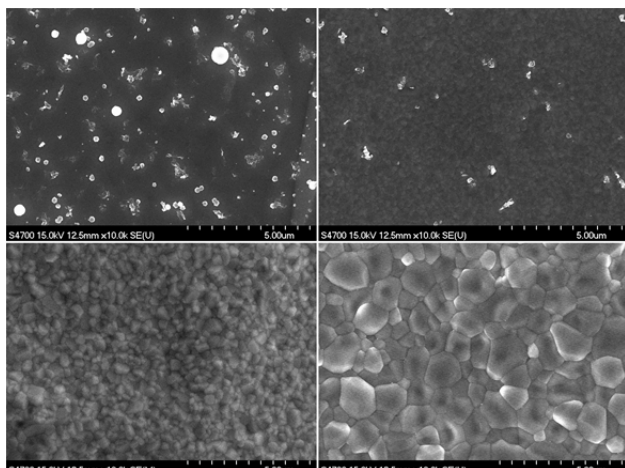
Figure 3: SEM images of BCPed samples at different stages of Nb$_3$Sn growth. The coating was stopped and the samples were removed from the furnace at four distinct stage of coating process: after one hour at 500 °C is in the top left, after one minute at 1200 °C is in the top right, after one hour at 1200 °C is in the bottom left, after three hours at 1200 °C is in the bottom right.



Figure 4: BL1 before and after Nb$_3$Sn coating. The cavity received mirror finish CBP, 800 °C x 2 hours, and 5 $\mu$m EP before the coating; note the shining appearance of polished niobium[left]. After the coating, the surface is matte gray characteristic of Nb$_3$Sn[right].

during RF tests indicated a high quality Nb$_3$Sn on the surface of tested cavities. For example, in Fig. 5, the average surface resistance as function of temperature is shown for ALD3, 1.5 GHz 1-cell cavity. The data fit is consistent with the energy gap of $\Delta_0 = 3.4$ meV. The transition temperature was measured in the same experiment to be $T_c$=17.9 K, Fig. 6. Hence, $2\Delta/k_B T_c$=2.2 indicates a strong coupling as expected for Nb$_3$Sn from earlier measurements. The 2-cell seamless cavities, used in our experiment, were centrifugally barrel polished (CBP) to a mirror finish(colloidal 0.04 $\mu$m silica with wooden blocks and water for about 120 hours), vacuum annealed at 800 °C for 2 hours, tuned for field flatness to 97 %, electropolished (EP) for 5 $\mu$m, and measured at 2.0 K before being prepared for the coating. The cavity performance at 2.0 K was typical of SRF niobium cavity with Q$_0$ of about $2\cdot10^{10}$ reaching at or above E$_{acc}$ = 20 MV/m. The cavities were then prepared for coating and coated as described in [13]. After the first coating, the cavities were stripped of Nb$_3$Sn with 5 $\mu$m EP. However, for two of the cavities 2-2 and 2-3, EPed together,
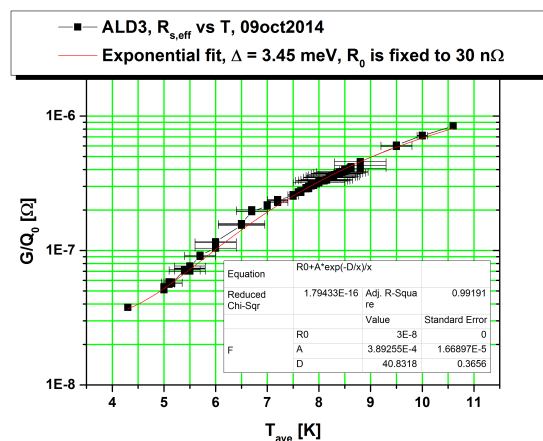


Figure 5: ALD3 RF surface resistance as a function of temperature. The line is the exponential fit to the data, from which the energy gap is calculated to be $\Delta = 3.4$ meV.

subsequent measurement at 2.0 K showed that the cavities have not recovered to the standard niobium performance. The other two cavities 2H3 and BL1 had performance similar to the 2.0 K test before coating. After re-baseline, 2H3 and BL1 were coated again under the same coating conditions.
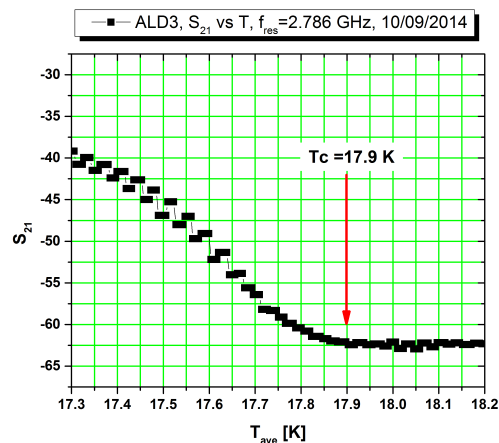


Figure 6: Measurement of the transmission through ALD3 as a function of temperature at f = 2.786 GHz. The measurement indicate a transition temperature of about 17.9 K.

In Fig. 7, 2H3 test results at 2.0 and 4.3 K after the first and second coatings are shown. After the first coating the cavity had a quality factor of about $10^{10}$ at both temperatures indicating that the surface resistance was dominated by the residual resistance term. The quench field was E$_{acc}$ = 3 MV/m at 4.3 K and E$_{acc}$ = 5 MV/m at 2.0 K. The temperature dependance of the quench field suggests that a weakly superconducting region dominated the performance of the cavity. After the second coating, the cavity quench field improved to E$_{acc}$ = 6 MV/m at 4.3 K and E$_{acc}$ = 10 MV/m at 2.0 K. The improvement in the quench field after the second coating is probably due to the 5 $\mu$m EP

that reduced the problematic region. While the quench field has changed, the quality factor between two coating is very consistent. The reproducibility of the coating procedure
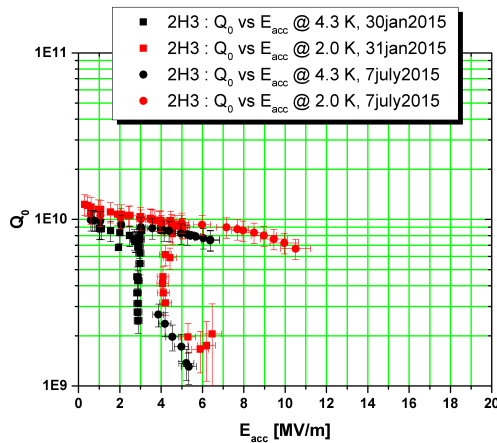


Figure 7: RF measurement of 2H3 after the first[squares] and second[circles] $Nb_3Sn$ coatings. Note that the quality factor is similar between two coatings at both 4.3 and 2.0 K. The improvement in the quench field after the second coating is probably due to reduction in the problematic region with 5 $\mu$m EP, which was done between the coatings.

was further demonstrated with BL1. In Fig. 8, BL1 test results after two coatings are shown. After the first coating, the cavity reached $E_{acc}$ above 10 MV/m at both 2.0 K and 4.3 K limited by a strong slope. The quality factor at 4.3 K was about $1.5 \cdot 10^{10}$ at $E_{acc} = 5$ MV/m. At 2.0 K the quality factor improved to $3 \cdot 10^{10}$ at $E_{acc} = 5$ MV/m. At this temperature the cavity reached $E_{acc} = 15$ MV/m limited by the available power and the cable heating. The second coating resulted in a very similar performance. We attribute the difference in $Q_0$ above $E_{acc}=8$ MV/m at 2.0 K between two measurement to the field emission that was observed in the second set of tests. These measurements showed the reproducibility of our coating procedure and that the variation in the cavity performance is likely due to the material properties and not due to uncontrolled variation in the preparation and coating procedures.

In Fig. 9 we summarize some of the single cell and two cell results at 2.0 K. Also, for comparison, some of the best results from Wuppertal and Cornell are included. This plot shows the cavities we coated and tested are limited by low field quenches and a reproducible Q-slope. The plot also clearly shows similarity between our results and the slope measured at Wuppertal University [9]. Had it not been for Cornell results in the same plot, the argument of fundamental limitation of $Nb_3Sn$ by a Q-slope would be supported by our results. However, the Cornell data clearly shows that the limitation can be overcome [11]. It is somewhat surprising to us that our data rather than Cornell's reproduces Wuppertal results, since, unlike Cornell, we did not adopt two heater approach in our coating setup and ran our coating in "Siemens" configuration [3]. Cornell on the other
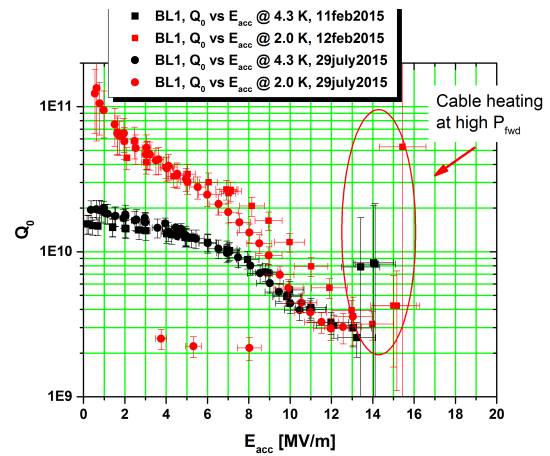
Figure 8: RF measurement of BL1 after the first[squares] and second[circles] $Nb_3Sn$ coatings. The quality factor field dependence is clearly reporducible from the first coating to the second. The variation the quality factor $E_{acc}=8$ MV/m at 2.0 K is likely due to field emission, which was observed in the test after the second coating.

hand has done their best to follow Wuppertal recipe, yet their cavity surpassed the slope to be limited by quench. The understanding of the cause for the slope as well as the
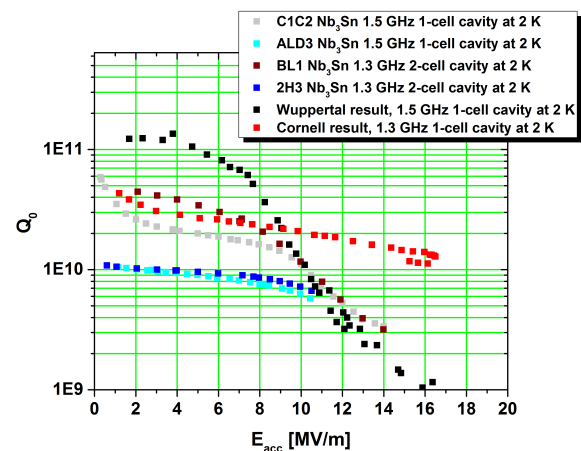


Figure 9: 2 K data for four coated cavities is shown. For comparison one of the best results from Wuppertal and Cornell are shown. Note that both our data and Wuppertal results [9] are limted by strong Q-slope, while Cornell's cavity [11] is not.

early quenches is necessary for improving of cavity performance. We have considered several possibilities for these limitations in our cavity. One possibility is the contamination of our coatings with Cl or Ti. As we mentioned earlier, the cavities were not built specifically for this project and were not all niobium cavities. They had NbTi flanges, which have been shown to result in Ti contamination after 1200 °C annealing [15]. Also, we are using a significantly higher amount of $SnCl_2$ in our process (3 gr cf. about 20 mg for Wuppertal/Cornell), which could also potentially be

a source of unwanted contamination. The other possibility is the variation in the coating composition. Since the diffusion-based process has to progress along concentration gradients, one would expect depth and lateral variations of Sn concentration.

## SURFACE STUDIES RESULTS

To understand the limitations in our cavities, we initiated materials studies on surfaces coated in our $Nb_3Sn$ coating system. The samples for analysis were either 1 cm x 1 cm niobium coupons cut with wire EDM from the 3 mm thick RRR niobium sheet used in cavity production, or cavity cutouts from C3C4 cavity, which was coated during $Nb_3Sn$ coating system commissioning. Note that C3C4 cavity was limited by a strong Q-slope at lower fields than the Wuppertal slope, and analysis of these samples provides insight into the surface conditions after typical coating process and also brings insight to the cause of the observed degradation.

In Fig. 10, SEM images of CVT-3 and CVT-4 samples are shown with a few characteristic features that were found. In the left picture, cracks can be seen on the coated surface. These cracks have been found in both cutouts, but never in the coated coupons. The cracks, Fig. 10 [left], extend tens of micrometer, and are all aligned in the same direction, which leads us to believe that they are caused by mechanical stress, possibly, during cutting out process, since we expects cracks caused by thermal stress to be randomly oriented. The other geometrical features that we found with SEM on the cutouts are voids between $Nb_3Sn$ grains, which could be the cause of the measured strong Q-slope, Fig. 10 [right].
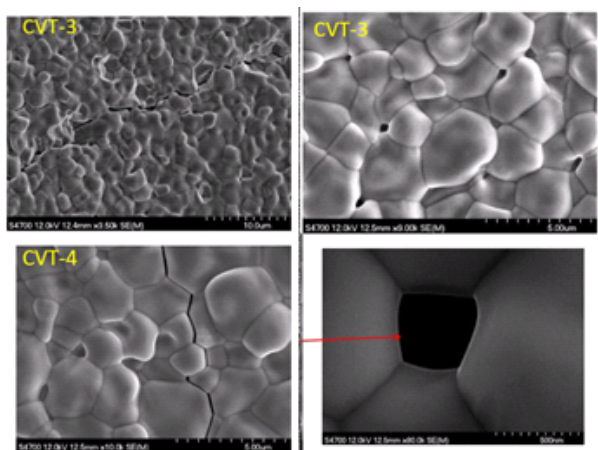


Figure 10: SEM images of the cavity cutouts, CVT-3 and CVT-4, from C3C4 cavity, which was coated during commissioning of our $Nb_3Sn$ coating system [12]. Pictures to the left show cracks on the surface, which extend tens of micrometers unidirectionally. Pictures to the right show voids in the coating.

Although the coupons have received the chemistry similar to niobium cavities, it was possible that the surface finish of the coupons was different from the cavity, and that

the topographical differences between coupons and cavity surface could cause the formation of voids and/or cracks. To explore this possibility we prepared several batches of coupons as received, BCPed, EP, or nanopolished. The samples then were coated at the same time with the standard coating procedure. Remarkably, the resulting coated surface looked very similar in SEM and AFM for all samples, Fig. 11 [16]. The quantitative analysis with surface
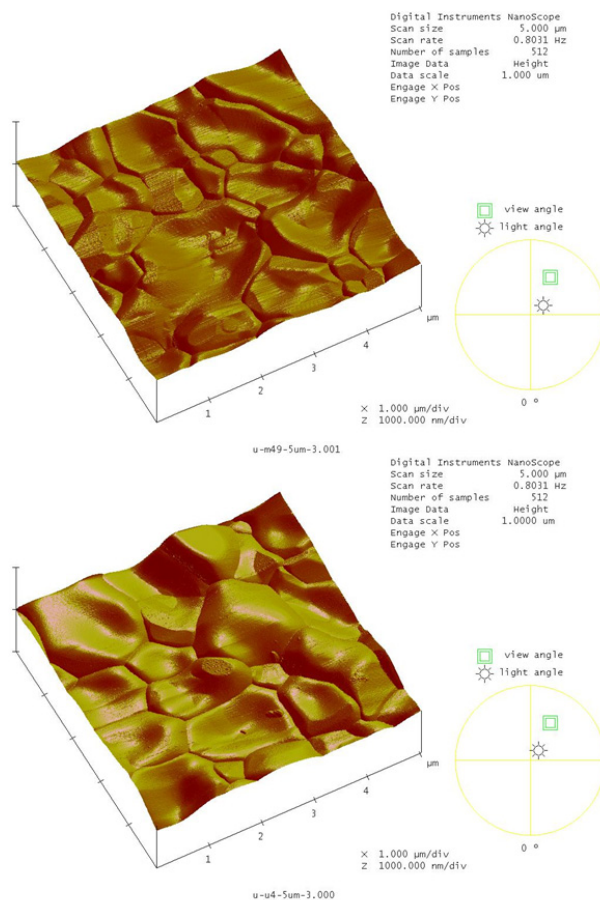


Figure 11: AFM scans of coated coated BCPed(M49, top) and nanopolished coupon(U4, bottom) niobium coupons. The lateral scale is 5 $\mu$m and the vertical scale is 1 $\mu$m for both samples. RMS roughness is 68 nm(M49) and 80 nm(U4) for this scan area.

height power spectral density (PSD) [17] indicates that the topography of the resulting surface is similar to the topography of BCPed niobium surface and is independent of the topography of the substrate, i.e., the resulting topography is the function of the coating process and not the original substrate surface, Fig. 12.

In Fig. 13 the EBSD map of the coated sample cross-section is shown. The map shows that the grains apparent in the SEM image are actually single crystals. The grain orientations appear to be random and uncorrelated to the adjacent grains or underlying niobium. It also shows that there is no indication of crystal orientation variation inside the grains. In this map, there is no evidence of lateral or
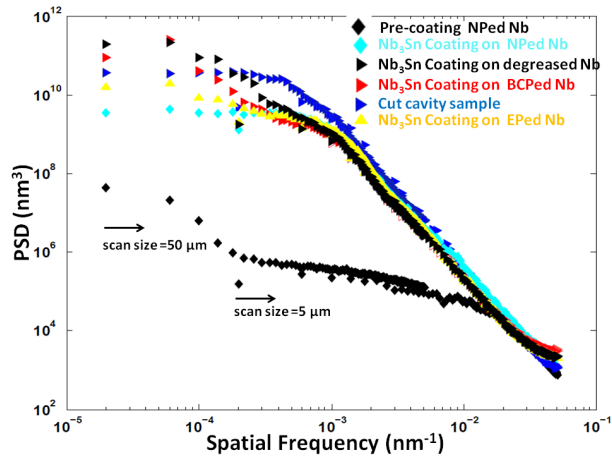
Figure 12: PSD analysis of AFM images collected from coated samples, which were prepared with different polishing techniques before coating. For comparison, PSD data a nanopolished niobium surface is shown [16].
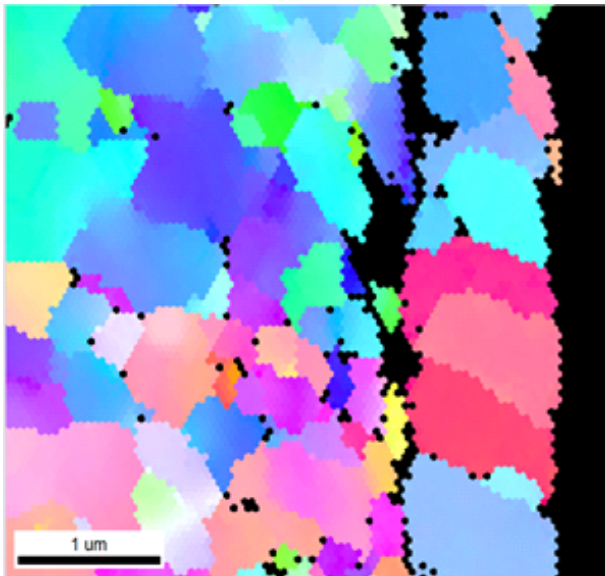


Figure 13: EBSD scan of the cross-section of a coated sample. The data indicates that grains apparent in SEM are single grains with the grain orientation being random and uncorrelated to the adjacent grains or underlying niobium grain [18].

depth compositional variation in the coated $Nb_3Sn$. The EBSD data is consistent with EDS measurement, which show that compositional variations in our $Nb_3Sn$ is within instrument sensitivity and reproducibility (24.3 ± 2) at. % [16]. We have not found significant variations in the $Nb_3Sn$ composition outside this range. To look for possible contamination in the coated films SIMS data was collected on some samples with a CAMECA IMS-7f magnetic sector instrument. The results as a function of depth is shown in Fig. 14. The data shows that $Nb_3Sn$ extend to the depth of about 1 $\mu$m with little variation in Nb and Sn concen-

trations. Carbon contamination is seen on the surface as expected for samples handled in air. We also see significant oxygen concentration in the $Nb_3Sn$ grain [18].
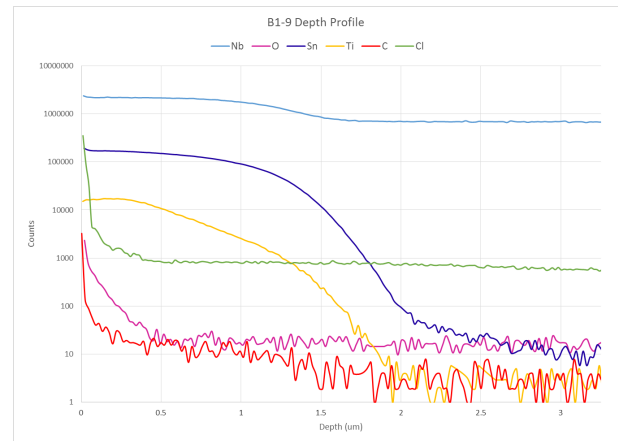


Figure 14: SIMS traces collected with CAMECA IMS-7f magnetic sector instrument.

SIMS results are further corroborated by XPS data, Fig. 15, which was collected on ULVAC-PHI "Quantera SXM". XPS survey scan indicates carbon present at the surface, as expected for samples exposed to ambient air, but no evidence of Cl is seen. High resolution XPS, Fig. 16, scan of Nb and Sn peaks shows that $Nb_3Sn$ is covered with $Nb_2O_5$ and $SnO_2$.
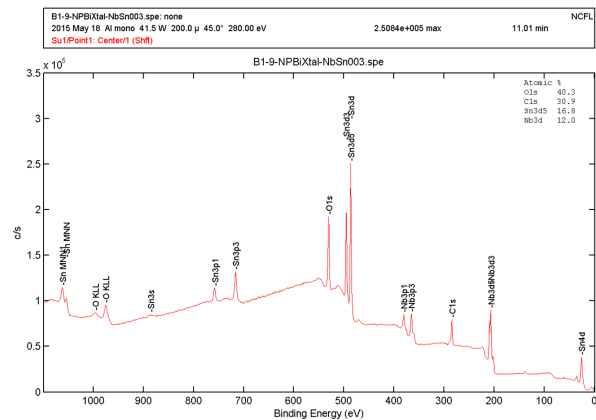


Figure 15: XPS survey scan. Note absence of Cl on the scan.

## CONCLUSION

Several 1.5 GHz 1-cell and 1.3 GHz 2-cell seamless cavities were coated with $Nb_3Sn$ and measured at 4.3 K and 2.0 K. The quality factors were typically about $10^{10}$ at 4.3 K and 2.0 K with several cavities reaching above $E_{acc}$ = 10 MV/m. The dominant limiting mechanisms were low field quenches and quality factor degradation above 8 MV/m, which is very similar to the slope observed at Wuppertal University [9]. The quality factor of the coated cavities was shown to be reproducible with re-coating, but varied
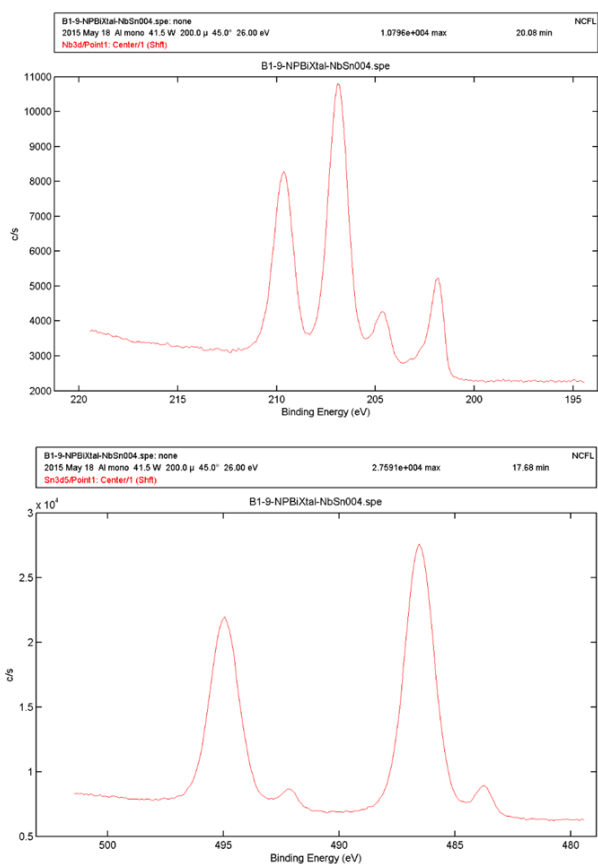
Figure 16: High resolution XPS scan data of Nb and Sn. The data is consistent with the individual oxides, $Nb_2O_5$ and $SnO_2$, on the surface.

from cavity to cavity. The energy gap and the transition temperature of coated cavities were found close the highest reported in the literature.

The EDS and SIMS surface analysis indicates a near-stoichiometric $Nb_3Sn$ consistent with the transition temperature and gap measurements. SEM images of the cutouts from the cavity coated during $Nb_3Sn$ coating system commissioning show voids and cracks that may have contributed to strong Q-degradation observed in the RF measurements. EBSD data show that the grains seen on SEM images are single crystal grains, which appear to be randomly oriented without correlation to adjacent grains or underlying substrate. XPS measurement show that $Nb_3Sn$ layer is covered with $Nb_2O_5$ and $SnO_2$ native oxides, and does not have Cl contamination on the surface. The typical grown films with our standard coating process are found to be about 2 $\mu$m thick and have a sharp boundary between the coated film and substrate.

Further studies are planned on the cavities, cavity cutouts, and coupons to investigate the outstanding issues of $Nb_3Sn$ coatings:

· Variation in coating quality due to the substrate;

· Quench limitations;

· Q-slope degradation.

## REFERENCES

[1] J. Charlesworth, I. MacPhail, and P. Madsen, J.Mat.Sci., 5:580 (1970).

[2] H. Devantay, J. Jorda, M. Decroux, J. Muller, and R. Fluekiger, J. Mater. Sci., 16:2145 (1981).

[3] B. Hillenbrand and H. Martens, Jour. Appl. Phys., 47(9):4151-4155 (1976).

[4] P. Kneisel, H. Kupfer, W. Schwarz, O. Stoltz, and J. Halbritter, IEEE Trans. Mag., 13(1):496-499 (1977).

[5] G. Arnolds, H. Heinrichs, R. Mayer, N. Minatti, H. Piel, and W. Weingarten, IEEE Trans. Nucl. Sci., 26(3):3775-3777 (1979).

[6] P. Kneisel, O. Stoltz, and J. Halbritter, IEEE Trans. Mag., 15(1):21-24 (1979).

[7] B. Hillenbrand, Y. Uzel, and K. Schnitzke, Appl. Phys. A, 23:237-240 (1980).

[8] James Stimmell, PhD dissertation, Cornell University, (1978).

[9] G. Muller, P. Kneisel, D. Mansen, H. Piel, J. Pouryamout, and R. W. Roth, Proc. EPAC'96, 3:2085-2087 (1996).

[10] P. Boccard, P. Kneisel, G. Mueller, J. Pouryamout, and H. Piel, Proc. SRF'97, 1094-1112 (1997).

[11] S. Posen, M. Liepe, and D. L. Hall, Appl. Phys. Lett. 106, 082601 (2015).

[12] G. Eremeev, W. Clemens, K. Macha, H. Park, R. Williams, Proc. IPAC'15, WEPI011, Richmond, U.S.A. (2015).

[13] G. Eremeev, Proc. IPAC'15, WEPWI010, Richmond, U.S.A. (2015).

[14] P. Kneisel and W. Singer, JLabTN14-012 (2012).

[15] P. Dhakal, G. Ciovati, G. R. Myneni, K. E. Gray, N. Groll, P. Maheshwari, D. M. McRae, R. Pike, T. Proslier, F. Stevie, R. P. Walsh, Q. Yang, and J. Zasadzinzki, Phys. Rev. ST Accel. Beams 16, 042001 (2013).

[16] U. Pudasaini et al., "Local Composition and Topography of Nb3Sn Diffusion Coatings on Niobium", these proceedings, TUPB054, SRF'15, Whistler, Canada (2015).

[17] Chen Xu, Hui Tian, Charles E. Reece, and Michael J. Kelley, Phys. Rev. ST Accel. Beams 14, 123501 (2011).

[18] J.Tuggle et al., "Structure and Composition of Nb3Sn Diffusion Coated Films on Nb", these proceedings, TUPB046, SRF'15, Whistler, Canada (2015).